Published in final edited form as:
Int J Parasitol. 2012 April ; 42(4): 411–419. doi:10.1016/j.ijpara.2012.03.001.

Giardia lamblia Nek1 and Nek2 kinases affect mitosis and excystation

Alias J. Smith[a,b], **Tineke Lauwaet**[a,*], **Barbara J. Davids**[a], and **Frances D. Gillin**[a]
[a]Department of Pathology, University of California, San Diego, CA, USA

Abstract

The NIMA-related serine/threonine kinases (Neks) function in the cell cycle and regulate ciliary and flagellar length. The *Giardia lamblia* genome encodes 198 Neks, of which 56 are predicted to be active. Here we believe that we report the first functional analysis of two *Giardia lamblia* Neks. The *Gl*Nek1 and *Gl*Nek2 kinase domains share 57% and 43% identity to the kinase domains of human Nek1 and Nek2, respectively. Both *Gl*Neks are active in vitro, have dynamic relocalization during the cell cycle, and are expressed throughout the life cycle, with *Gl*Nek1 being upregulated in cysts. Over-expression of inactive *Gl*Nek1 delays disassembly of the parental attachment disk and cytokinesis, while over-expression of either wild type *Gl*Nek1 or inactive mutant *Gl*Nek2 inhibits excystation.

Keywords

Giardia; Nek; Kinase; Mitosis; Excystation

1. Introduction

Giardia lamblia (synonymous with *Giardia intestinalis* and *Giardia duodenalis*) remains a major cause of water-borne diarrheal disease and food-borne illness worldwide (Kramer et al., 1996; Adam, 2001; Savioli et al., 2006; Budu-Amoako et al., 2011). The pathogenesis of this protozoan parasite depends on its biphasic lifecycle (Boucher and Gillin, 1990). Upon ingestion, dormant giardial cysts pass through the stomach where they are activated by gastric acid, although the parasites are protected by the cyst wall. Once the parasites reach the small intestine they rapidly exit the cyst wall, producing four trophozoites after two rounds of cell division. Trophozoites are characterized by their half-pear shape, two nuclei, eight flagella, each anchored by a basal body, and ventral attachment disk. While maintaining infection of the small intestine, parasites divide by binary fission. This cell division involves nuclear duplication, flagellar maturation and segregation, parental disk disassembly and daughter disk assembly (Nohynkova et al., 2006; Tumova et al., 2007; Dawson and House, 2010). Cell division is believed to be a rapid process as a functional cytoskeleton is required for attachment. Parasites that are swept downstream can sense the change in the environment and begin to encyst, which involves cytoskeletal rearrangements, reduced metabolism and motility, and formation of encystation secretary vesicles (ESVs)

[*]Corresponding author. Tineke Lauwaet, Department of Pathology, 214 Dickinson Street, CTF-C, University of California at San Diego, San Diego, CA, 92103-8416, USA, Tel.: +1 619 543 7729; fax: +1 619 471 9439. tlauwaet@ucsd.edu.
[b]Current address: Department of Oncology, Georgetown University, 3970 Reservoir Rd NW, Washington DC 20007, USA

that export cyst wall components to the plasma membrane (Reiner et al., 1990; Marti et al., 2003; Palm et al., 2005). Mature cysts exit the host in feces and survive in fresh water, waiting to complete the infection cycle.

The molecular signaling pathways that ensure accurate spindle formation, chromosome segregation and final cell division during the giardial cell and life cycle, remain incompletely understood (Abel et al., 2001; Nohynkova et al., 2006; Dawson et al., 2007; Lauwaet et al., 2007; Davids et al., 2008; Alvarado and Wasserman, 2010). The four major mitotic kinase families that control eukaryotic chromosomal segregation during the cell cycle are Never in Mitosis Gene A-related (Nek), Aurora, Polo and cyclin-dependent kinases, (all with members that localize to the centrosomes/basal bodies of mammalian cells) (Malumbres and Barbacid, 2007). To date Aurora Kinase (AK) is the only kinase shown to be involved in the giardial cell cycle. AK is activated and localizes to the basal bodies and spindle microtubules during mitosis (Davids et al., 2008). The lone giardial member of the Polo kinase family, Plk1, was localized to the flagellar basal bodies (Morrison et al., 2007; Lauwaet et al., 2011; Manning et al., 2011).

Neks are known as regulators of the eukaryotic cell cycle and certain members of this family have been implicated in driving G2-M progression (Fry, 2002; Quarmby and Mahjoub, 2005; O'Regan et al., 2007; Liu et al., 2010; Chen et al., 2011a). Human Nek1 is reported to have a role in controlling meiotic events and mutations are implicated in polycystic kidney disease (Liu et al., 2002; Mahjoub et al., 2004; Shalom et al., 2008). The mammalian Nek1 is also involved with DNA damage sensing and repair, mitotic chromosome segregation and cytokinesis (Chen et al., 2011a, 2011b). Human Nek2 is the best-characterized member of the mammalian Nek family and has been described to regulate mitotic commitment, centriole splitting and promote proper kinetochore-microtubule connections (Chen et al., 2002; Fry, 2002; DeLuca et al., 2003; Faragher and Fry, 2003; Lou et al., 2004; Du et al., 2008). Over-expression of active *Hs*Nek2 in 293T cells leads to premature splitting of mother and daughter centrioles before the G2/M transition, resulting in the inhibition of mitotic onset (Fry, 2002; Liu et al., 2010). Additionally, during mitosis *Hs*Nek2 is essential for efficient kinetochore microtubule attachment and faithful chromosome segregation (Faragher and Fry, 2003; Lou et al., 2004; Fu et al., 2007; Du et al., 2008). Humans have 11 members of the Nek family, while *Plasmodium falciparum, Chlamydomonas reinhardtii, Trypanosoma brucei, Leishmania major* and *Tetrahymena thermophila* encode four, 11, 12, 13 and 39 Neks, respectively. In general, ciliated or flagellar organisms possess more members of the Nek family (Quarmby and Mahjoub, 2005; Parker et al., 2007). The *Giardia* genome encodes 198 Neks, which is strikingly more than any other reported organism (Morrison et al., 2007; Manning et al., 2011). Proteomic analysis of giardial mitosomes and a basal body enriched fraction identified six and 11 Neks, respectively. Localization studies have confirmed two of the Neks (Gl50803_16279 and GL50803_92498) to be basal body-associated proteins (Lauwaet et al., 2011), while several other Neks are either primarily cytoplasmic (Gl50803_101534 and Gl50803_15409) or associate with the anterior and caudal axonemes (Gl50803_5375) (Manning et al., 2011). The increased number of giardial Neks may be needed for the complex processes of flagellar maturation, cytoskeletal rearrangements and faithful chromosome segregation during the cell and life cycles (Nohynkova et al., 2006; Dawson et al., 2007; Parker et al., 2007; Tumova et al., 2007).

In this study, we characterized the two giardial Neks that share highest sequence identity with the kinase domains of human Nek1 and Nek2 and studied their roles in the cell and life cycles. Our study shows that these kinases are involved in regulating cell division and excystation.

2. Materials and methods

2.1. HMMER search of genome

The dataset containing the predicted proteins of *Giardia lamblia* Assemblage A isolate WB was downloaded from http://giardiadb.org (release-2.5). The single sequence query JackHMMER program (Johnson et al., 2010) was used to query the protein dataset for the presence of human Nek1 (Swiss-Prot, Q96PY6) and human Nek2 (Swiss-Prot, P51955). The inclusion threshold was set at 0.001.

2.2. Cell culture, encystation and excystation

Giardia trophozoites were cultured in modified TYI-S-33 medium with bovine bile (Keister, 1983), with encystation (Davids et al., 2011) and excystation induced as previously described (Keister, 1983; Boucher and Gillin, 1990). At 21 h encystation, the numbers of ESV were counted in live trophozoites using differential interference contrast optics. Cysts were collected after 48 h encystation from the bottom of the culture flasks and remaining trophozoites were lysed by incubation in double-distilled water for 20 min at 4°C. Water-resistant cysts were washed three times, counted and stored overnight in double-distilled water at 4°C. In Stage 1 of excystation, cysts were exposed to an acidic-reducing solution (57 mM L-cysteine HCl, 32.5 mM reduced glutathione, 0.1 M NaHCO3, in Hank s balanced salt solution, pH 2.0) for 30 min at 37°C. In Stage 2, acid-treated cysts were washed and treated with trypsin in pH 8.0 bicarbonate-buffered Tyrode s solution for 1 h at 37°C. Finally, excysting cysts were transferred to regular growth medium for 60 min at 37°C. The numbers of excyzoites were counted in three independent experiments. Simple one-way ANOVA was used to determine significance among excyzoite counts.

2.3. Epitope tagging of GlNeks

The promoter and coding region of *Gl*Nek1 and *Gl*Nek2 were amplified from 200 ng of *G. lamblia* genomic DNA using primers “GlNek1-Apa1-for” (5′-GGGCCCCCGGATGCGCGTCTGTTG-3′), “GlNek1-EcoRV-rev” (5′-GATATCCCTGACAGTATTGAACCTGTCC -3′), “GlNek2-Apa1-for” (5′-taagggccccagcatctagctgaatgccga-3′), and “GlNek2-EcoRV-rev” (5′-taagatatccatcttatacttgtaagcgcc-3′). The PCR products and a vector encoding the C-terminal HA tag were digested with *Apa*I and *Eco*RV. The digested PCR products and vector were gel extracted using a QIAquick Gel Extraction Kit (Qiagen, USA) and ligated overnight at 16°C. The targeted mutations, *Gl*Nek1 K22M (KM) and *Gl*Nek2 K64M, were introduced using the QuikChange site-directed mutagenesis method (Stratagene, USA). All plasmids were sequenced to confirm the presence of the desired mutation (Etonbio, USA). *Gl*Nek1 and *Gl*Nek2 over-expression plasmids were created by subcloning the Nek coding sequences from the wild type (WT) and mutant HA tag plasmids described above into the vector with the ornithine carbamoyl transferase (OCT) promotor using the primers 5′-CTCGAGATGGAACGCTACAAGGAGCTTAAGG-3′ for *Gl*Nek1, 5′-CTC GAGATGGCCAACGCAGGCGGACGAC-3′ for *Gl*Nek2, and the universal reverse primer 5′-GGGCCCCCTAAGTCGGATCCCTATGCATAGTCTGG-3′ (to include the 3xHA tag from the HA vector). The PCR products and the OCT over-expression vector were digested with *Xho*I and *Apa*I, gel extracted (Qiagen) and ligated overnight at 16°C. All plasmids were transformed into *E. cloni* 10G competent cells (Lucigen USA). DNA was purified from overnight bacterial cultures using a Maxiprep kit (Qiagen) and sequenced (Etonbio). Trophozoites were electroporated with 50 μg of plasmid DNA and transfectants were maintained through puromycin selection.

2.4. Cellular localization of GlNek1 and GlNek2

Localization of *Gl*Nek1 and *Gl*Nek2 during mitosis was assessed by IFA. Parasites were grown on coverslips in anaerobic chambers to enrich for adherent mitotic cells. The cells were fixed for 10 min in cold methanol (−20°C), dried, permeabilized in 0.5% Triton-X 100 for 10 min, and blocked for 1 h in block solution (10% goat serum, 1% glycerol, 0.1% BSA, 0.1% fish gelatin and 0.04% sodium azide in PBS). The coverslips with fixed parasites were incubated with 1/500 mouse anti-phosphorylated Aurora Kinase A (pAK) antibody (Abcam, USA) for 1 h, washed with PBS, incubated with 1/100 anti-HA-FITC and 1/800 goat-anti-mouse-Alexa, and washed four times with PBS. All antibodies were diluted in block solution. Cells were post-fixed with 4% paraformaldehyde, rinsed and mounted with Prolong Gold with DAPI (Molecular Probes, USA). Fluorescence was observed and photographed on a Nikon Eclipse E800 microscope equipped with an X-Cite™ 120 fluorescence lamp and 1000x magnification (Nikon Instruments Inc., USA).

2.5. Expression and purification rGlNek1 and GlNek2

The genes encoding *Gl*Nek1 (GL50803_92498) and *Gl*Nek2 (GL50803_5375) were cloned into the bacterial expression vector pETite C-His (Lucigen) using the primers 5′-GAAGGAGATATACATATGGAACGCTACAAGGAGCTTAAGG-3′ and 5′-GTGATGGTGGTGATGATGCCTGACAGTATTGAACCTGTCC-3′ for *Gl*Nek1, and 5′-GAAGGAGATATACATATGGCCAACGCAGGCGGACGAC-3 and 5′-GTGATGGTGGTGATGATGCATCTTATACTTGTAAGCGCC-3′ for *Gl*Nek2. The targeted mutations, *Gl*Nek1 K22M and *Gl*Nek2 K64M, were introduced using the QuickChange site-directed mutagenesis method (Stratagene). All plasmids were sequenced to confirm the desired mutations (Etonbio). The four resulting vectors were individually transformed into Hi-Control BL21(DE3) cells and cells were induced with 1 mM IPTG to express WT or mutant His-tagged *Gl*Nek1 and *Gl*Nek2. WT and mutant GlNeks were purified from induced bacterial lysates using HisExpress columns (Claremont Biosolutions, USA) according to the manufacturer's recommendations.

2.6. Western blot analysis

Proteins from trophozoites and cysts were precipitated with trichoroacetic acid (TCA), separated on 4–20% Tris-glycine gels and transferred as previously described (Lauwaet et al., 2007). Filters were blocked for 1 h in 5% milk in PBS supplemented with 0.1% Tween-20 (PBST), incubated for 1 h in 5% milk in PBST with anti-His-HRP (horseradish peroxidase; Bethyl, USA) or anti-HA-HRP (Roche, USA). Filters were washed and the signal was developed with ECL-Plus (GE Healthcare, USA). As a protein loading control, filters were re-probed with an antibody against taglin (Ward et al., 1987).

2.7. Kinase assay

Kinase reactions (60 μl) were performed in kinase buffer (20 mM Tris-HCl pH 7, 20 mM $MgCl_2$, 2 mM $MnCl_2$, 165 μM ATP (Invitrogen), 300 nM recombinant WT or mutant GlNek1 or GlNek2, and 125 ng/μl recombinant human Histone H1 (New England BioLabs, USA), recombinant human Histone H3 (New England BioLabs), or BSA (Invitrogen). The reactions were incubated at 30°C for 45 min and stopped by adding 12 μl of 6X reducing Laemmli sample buffer and heating for 5 min at 100 °C. Kinase reactions (15 μl) were resolved on two 14% SDS-PAGE gels. The first set of gels was fixed, stained with ProQ Diamond (Invitrogen), destained and imaged as directed by the manufacturer s recommendations. The intensity of the observed bands was quantified with the ImageJ software. After imaging, these gels were stained with Coomassie Brilliant Blue to assess total protein content of the kinase reactions. The duplicate 14% SDS-PAGE gels were

transferred to polyvinylidene fluoride (PVDF) membranes and processed for western blotting with the anti-His-HRP antibody.

3. Results

3.1. GlNek1 and GlNek2 are homologous to active NIMA-related kinases (Neks)

We used JackHMMER searches and the human *Hs*Nek1 and *Hs*Nek2 protein sequences to query the sequences in the *G. lamblia* genome. Our searches identified GL50803_92498 and GL50803_5375 as the closest hits with 57% and 43% identity to *Hs*Nek1 and *Hs*Nek2, respectively, within the kinase domains. We will refer to the proteins encoded by GL50803_92498 as *Gl*Nek1 and by GL50803_5375 as *Gl*Nek2. *Gl*Nek1 is 898 amino acids in length and is predicted to be ~102 kDa, while *Gl*Nek2 is 405 amino acids in length and is predicted to have a mass of ~45 kDa. Outside of the conserved kinase domain, *Gl*Nek1 has two coiled-coil domains and one PEST domain, while *Hs*Nek1 contains five coiled-coil domains and three PEST domains (Fig. 1A). *Gl*Nek2 has one coiled-coil domain, but no PEST domain. *Hs*Nek2 has a similar predicted mass (~51 kDa) to *Gl*Nek2, and also has one coiled-coil domain. *Gl*Nek1 and *Gl*Nek2 lack additional domains that are found in *Hs*Nek2: one KEN-box domain, one D-Box domain, a leucine zipper motif and a protein phosphatase 1 binding site (Fig. 1A). PEST, KEN-box and D-box domains are common features of proteins targeted for rapid degradation (King et al., 1996; Rechsteiner and Rogers, 1996; Barford, 2011). Both putative giardial kinases are predicted to be active based on the presence of all conserved serine/threonine kinase sub-domains, including the glycine loop that anchors the non-transferable ATP phosphates, the invariant lysine (K33 in *Hs*Nek1) that is required for maximal activity, and the DFG triplet that helps orient the ATP gamma-phosphate for transfer (Fig. 1B) (Hanks and Hunter, 1995).

3.2. GlNek1 and GlNek2 are active kinases in vitro

To determine whether *Gl*Nek1 and *Gl*Nek2 are active kinases, we expressed each in *Escherichia coli* as a C-terminal 6His-tagged protein and tested their activity with a standard kinase assay. Recombinant *Gl*Nek1 (r*Gl*Nek1-WT) and *Gl*Nek2 (r*Gl*Nek2-WT) were able to phosphorylate recombinant human histone H1 (H1), as indicated by the higher signal intensity compared with the background signal of the H1 substrate alone (Fig. 2A and B). r*Gl*Nek1-WT, but not r*Gl*Nek2-WT, phosphorylated recombinant human histone H3 (H3), while r*Gl*Nek2, but not r*Gl*Nek1, phosphorylated BSA. Mutated r*Gl*Nek1-KM and r*Gl*Nek2-KM, which have a methionine instead of the invariant lysine in sub-domain II of the kinase domain had no detectable kinase activity. This rules out the possibility that the kinase activity was due to bacterial contamination of the purified Neks. From these data we conclude that under these conditions, r*Gl*Nek1-WT and r*Gl*Nek2-WT are active kinases that display different preferences towards the artificial substrates tested. Moreover, the invariant lysine in subdomain II is necessary for kinase activity, as observed with human Nek2, trypanosome *Tb*NRKC and plasmodial Nek2 (Fry et al., 1995; Pradel et al., 2006; Reininger et al., 2009).

3.3. GlNek1 and GlNek2 have dynamic localization during mitosis

During interphase, *Gl*Nek1 localizes to the basal bodies, ventral disk, median body, anterior paraflagellar dense rods (PFR) and/or axonemes, and intracellular portions of the caudal and posterior-lateral axonemes (Fig. 3) (Lauwaet et al., 2011; Manning et al., 2011). During mitosis AK is activated by phosphorylation and is a valuable marker for identifying and characterizing cells in the progressive stages of mitosis (Davids et al., 2008). To identify Nek localization throughout mitosis, we double stained cells expressing HA-tagged *Gl*Nek1 or *Gl*Nek2 (*Gl*Nek1-WT and *Gl*Nek2-WT) under their own promoter with anti-HA and an antibody against the phosphorylated form of Aurora Kinase (anti-pAK). *Gl*Nek1-WT has a

dynamic localization pattern throughout mitosis, similar, although not identical, to that observed for pAK (Fig. 3). The characteristic *Gl*Nek1-WT staining in the anterior PFR/axonemes (Fig. 3, white arrow) decreases from interphase to metaphase, where it is no longer detected. This is likely due to the internalization and re-localization of the anterior flagella during the cell cycle (Nohynkova et al., 2006). Like pAK, *Gl*Nek1-WT localizes to the re-organized basal bodies, some of which form the spindle poles, during metaphase and anaphase (Fig. 3, red arrow). *Gl*Nek1-WT and pAK both localize to the unfolding parental disk, which disassembles during cytokinesis. Overall, *Gl*Nek1-WT partially co-localizes with pAK during mitosis, with several areas of the cells being more strongly stained by either pAK (i.e. the area around the nuclei in prophase and spindle fibers in metaphase) or anti-HA (*Gl*Nek1-WT) (i.e. median bodies in prophase and metaphase) depending on the stage of mitosis.

*Gl*Nek2-WT localizes to the anterior and caudal flagellar axonemes during interphase (Manning et al., 2011) (Fig. 4, white arrow). Similar to *Gl*Nek1-WT, *Gl*Nek2-WT localization to the anterior PFR and axonemes is less intense in metaphase compared with interphase cells. During metaphase and anaphase, *Gl*Nek2-WT localizes to the spindle poles (Fig. 4, red arrow) and spindle microtubules, similar to pAK. During telophase and cytokinesis, *Gl*Nek2-WT is primarily observed in the developing daughter anterior PFR and axonemes (Fig. 4, white arrows). Unlike pAK and *Gl*Nek1-WT, *Gl*Nek2-WT is not readily detected in the disassembling parental disk.

3.4. Over-expression of kinase dead GlNek1 or GlNek2 leads to mitotic defects

To assess whether *Gl*Nek1 and *Gl*Nek2 are involved in *Giardia* growth, we over-expressed both WT and KM *Gl*Nek1 and *Gl*Nek2 under the highly active OCT promoter and compared the growth rate of these cell lines with the growth of a control cell line with an empty expression vector (OCT-empty). Over-expression was confirmed by western blot (Supplementary Fig. S1). A slightly higher molecular weight band was observed in the *Gl*Nek1-OCT-KM sample, which may be the result of post-translational modification, such as phosphorylation. Cells expressing either *Gl*Nek1-OCT-WT or *Gl*Nek1-OCT-KM have significantly decreased growth rates, and cell lines expressing *Gl*Nek2-OCT-WT and *Gl*Nek2-OCT-KM have an even more pronounced growth defects (Fig. 5A). The localization of *Gl*Nek1-WT and KM, from interphase to telophase, in the over-expressing cell lines was the same as in the cell lines expressing endogenous *Gl*Nek1-WT levels (data not shown). However, approximately 50% of *Gl*Nek1-OCT-KM cells in cytokinesis appeared to be delayed in cytokinesis as evidenced by their intact parental disk outlined by pAK staining (Fig. 5B, “Stalled Cytokinesis”, green arrows). The remaining ~50% of *Gl*Nek1-OCT-KM cells in cytokinesis displayed the wild type localization of *Gl*Nek1 and pAK (Fig. 5B, “Progressing Cytokinesis”). In the “Stalled Cytokinesis” sub-population of cells, *Gl*Nek1-OCT-KM localized to the daughter disks, basal bodies, anterior PFR and axonemes, median body and intracellular portions of the caudal and posterior-lateral axonemes of the daughter cells. This indicated that the daughter cells are nearly fully formed. More dorsally focused images of the cells (Fig. 5B) did not reveal the presence of pAK labeled basal bodies or spindle microtubules, confirming that the cells are indeed in cytokinesis and not telophase (data not shown). Cell counts of live cultures revealed that ~39% of cells over-expressing the mutant form of *Gl*Nek1 were in cytokinesis compared with ~6 and ~7% in the C6 parental and OCT empty vector control cell lines, respectively (Fig. 5C). No significant differences were found among the cell lines expressing *Gl*Nek1-OCT-WT, *Gl*Nek2-OCT-WT, or *Gl*Nek2-OCT-KM. The significant increase in cells expressing *Gl*Nek1-OCT-KM in cytokinesis correlates with the phenotype observed by immunofluorescence, and further indicates that endogenous *Gl*Nek1 may have a role in regulating the disassembly of the parental disk. The growth defects of parasites over-

expressing wild type *Gl*Nek1 or *Gl*Nek2 or mutant *Gl*Nek2 were not associated with any obvious morphological changes revealed by immunocytochemistry.

3.5. Over-expression of wild type GlNek1 or mutant GlNek2 inhibits excystation

To determine whether *Gl*Nek1 or *Gl*Nek2 have roles in regulating the giardial life cycle, we first tracked the endogenous protein expression levels of *Gl*Nek1-WT and *Gl*Nek2-WT in lysates of vegetative, encysting and excysting cells. Western blots show that the expression of *Gl*Nek1-WT dropped slightly during encystation and increased ~3.4 and ~2.4 fold in cysts and excystation stage 1 (S1), respectively, relative to the vegetative level of expression (Fig. 6A). The protein expression of *Gl*Nek2-WT increased ~1.7 fold during encystation through S1, relative to vegetative expression. Expression of both *Gl*Neks decreased below vegetative levels during stage 2 of excystation. The protein expression of both *Gl*Neks correlated well with the mRNA expression levels in the life cycle as shown by Serial Analysis of Gene Expression (SAGE) (www.giardiadb.org).

We next assessed the ability and efficiency of cell lines over-expressing WT or KM *Gl*Nek1 and *Gl*Nek2 to encyst and excyst in vitro. There were no significant differences in the numbers of ESVs and cysts, relative to the parental and OCT-empty vector control cell lines (data not shown). However, water-resistant cysts from parasites expressing *Gl*Nek1-OCT-WT and *Gl*Nek2-OCT-KM both released ~ 50% fewer excyzoites than the cysts derived from the OCT-empty control (Fig. 6B). Cysts from *Gl*Nek1-OCT-KM and *Gl*Nek2-OCT-WT cell lines excysted equally as well as the OCT- empty-vector control cysts. These data indicate that excess WT *Gl*Nek1 can be deleterious to excystation and that the kinase activity of *Gl*Nek2 is necessary for efficient excystation.

4. Discussion

The giardial Nek kinase family is dramatically expanded (Morrison et al., 2007; Lauwaet et al., 2011; Manning et al., 2011), and there is a significant likelihood that several functional redundancies will be identified in future studies. However, the C- terminal domains of most of the 198 giardial Neks are highly divergent (Manning et al., 2011), indicating that these kinases can have unique protein-protein interactions, substrate specificities and cellular localizations, leading to a wide array of potential signaling functions. *Gl*Nek1 and *Gl*Nek2 share high sequence identity only within their kinase domains and significant overall domain architecture similarity to human *Hs*Nek1 and *Hs*Nek2, respectively. Both giardial Neks possess the conserved sub-domains required for serine/threonine kinase activity and our experiments validated this prediction. In interphase cells, both *Gl*Nek1 and *Gl*Nek2 localize to cytoskeletal structures, including the anterior and caudal axonemes, with *Gl*Nek1 additionally localizing to the basal bodies, median bodies, attachment disk and posterior-lateral axonemes. During the cell cycle, both *Gl*Nek1 and *Gl*Nek2 have dynamic localization patterns and target to the spindle poles (*Gl*Nek1 and *Gl*Nek2), the spindle microtubules (*Gl*Nek2) and the disassembling parental disk (*Gl*Nek1), suggesting they might have distinct functions during mitosis.

To assess the function of *Gl*Nek1 we over-expressed its active WT and inactive KM forms in *Giardia*. Both *Gl*Nek1-OCT-WT and *Gl*Nek1-OCT-KM over-expressing lines had growth deficiencies and a subset of *Gl*Nek1-OCT-KM cells stalled during cytokinesis. In contrast to *Gl*Nek1-OCT-WT cells, ~50% of the heart-shaped, dividing *Gl*Nek1-OCT-KM cells had parental disks that failed to disintegrate, likely inhibiting these cells from completing cytokinesis (Fig. 5B). This indicated that the kinase activity of the endogenous *Gl*Nek1 is likely involved in regulating the normal disassembly of the parental disk during cell division. Proper formation of the ventral disk is critical for trophozoites to complete cytokinesis and maintain infection (Tumova et al., 2007). Our data place *Gl*Nek1 in the

correct location to influence ventral disk microtubule dynamics and indicate that *Gl*Nek1 may act as a positive regulator of parental disk microtubule disassembly. If this is the case, over-expression of active wild type *Gl*Nek1 would lead to premature disassembly of the parental disk or delayed assembly of the daughter disks during telophase, both of which could result in the decreased growth rate. In summary, our data suggest that an imbalance of both active and inactive *Gl*Nek1 affects growth and cytokinesis.

Of the 198 giardial Neks, the sequence of *Gl*Nek2 is most similar to that of *Hs*Nek2. Expression of either *Gl*Nek2-OCT-WT or *Gl*Nek2-OCT-KM led to greatly decreased growth rates. Similar to *Hs*Nek2, the over-expression of active or inactive *Gl*Nek2 could result in reduced growth due to inhibition of mitotic onset (active) or inaccurate chromosome segregation (inactive) (Fry, 2002; Liu et al., 2010).

We next assessed the potential functions of *Gl*Nek1 and *Gl*Nek2 during the life cycle. We did not observe any significant effects on encystation of cell lines over-expressing active or inactive *Gl*Nek1 or *Gl*Nek2. However, *Gl*Nek1-OCT-WT and *Gl*Nek2-OCT-KM cysts were significantly reduced in their capacity to excyst. Our growth and localization data suggest that *Gl*Nek1 helps to regulate disassembly of the parental disk. Hence, cells over-expressing active *Gl*Nek1 may be less able to assemble new daughter disks (Tumova et al., 2007), resulting in fewer excyzoites. Since disk disassembly is not necessary until the second round of excyzoite division, it is not surprising that *Gl*Nek1-OCT-KM cells defective in disk disassembly had no phenotype in early excystation. For *Gl*Nek2, we saw the opposite effect: cells over-expressing KM *Gl*Nek2 but not the WT *Gl*Nek2 showed reduced excystation. Similar to HsNEK2, *Gl*Nek2 may be involved in accurate chromosome segregation through regulation of kinetochore microtubules. During excystation, the 4 N content of each of the nuclei in the emerging excyzoite must be properly segregated twice to yield four trophozoites containing the correct DNA content (Bernander et al., 2001). Since *Gl*Nek2 localizes to the basal bodies, over-expression of inactive *Gl*Nek2-OCT-KM could inhibit activation of proteins necessary to properly connect the kinetochore microtubules to the chromosomes. This would adversely affect the accurate segregation of the chromosomes, resulting in non-viable excyzoites. Over-expression of *Hs*Nek2 adversely affects mitotic entry of 293T cells (Liu et al., 2010), however over-expression of *Gl*Nek2 did not inhibit the emergence and division of early excyzoites. Most likely, excyzoites that emerge from cysts are already past the mitotic commitment checkpoint, given their 16 N state. In this case, over-expressing *Gl*Nek2-OCT-WT would not inhibit the first round of cell division of excystation. Over-expression of the kinase-dead mutant *Gl*Nek1 and *Gl*Nek2 likely interferes with native *Gl*Nek signaling through sequestering upstream activating kinases and/or substrates in kinase inactive complexes.

We identified two members of the *Giardia* Nek family that are likely to have distinct functions during the giardial cell cycle and life cycle: *Gl*Nek1 in regulating the microtubule dynamics of the ventral disk and *Gl*Nek2 in regulating mitotic commitment and/or fidelity of chromosome distribution to daughter parasites. Our studies of these two giardial Neks begin to reveal the diversity of their expression, localization, kinase activity and function in growth and differentiation. Additional studies are needed to elucidate the complexity of the signaling pathways of these and other *Gl*Neks and to help understand the striking expansion of these kinases in *Giardia*.

Supplementary Material

Refer to Web version on PubMed Central for supplementary material.

Acknowledgments

We thank Nathan Low, Nele Nijs, Maya Millman-Gray and Cynthia Quindoza for excellent technical support and Dr. Heidi Elmendorf for additional support and guidance. This work was supported by National Institutes of Health (NIH), USA, grants AI42488 and AI75527. AJS was supported by the Gastroenterology Training Program, T32 DK007202.

References

Abel ES, Davids BJ, Robles LD, Loflin CE, Gillin FD, Chakrabarti R. Possible roles of protein kinase A in cell motility and excystation of the early diverging eukaryote *Giardia lamblia*. J Biol Chem. 2001; 276:10320–10329. [PubMed: 11104758]

Adam RD. Biology of *Giardia lamblia*. Clin Microbiol Rev. 2001; 14:447–475. [PubMed: 11432808]

Alvarado ME, Wasserman M. Analysis of phosphorylated proteins and inhibition of kinase activity during *Giardia intestinalis* excystation. Parasitol Int. 2010; 59:54–61. [PubMed: 19861170]

Barford D. Structural insights into anaphase-promoting complex function and mechanism. Philos Trans R Soc Lond B Biol Sci. 2011; 366:3605–3624. [PubMed: 22084387]

Bernander R, Palm JE, Svard SG. Genome ploidy in different stages of the *Giardia lamblia* life cycle. Cell Microbiol. 2001; 3:55–62. [PubMed: 11207620]

Boucher SE, Gillin FD. Excystation of in vitro-derived *Giardia lamblia* cysts. Infect Immun. 1990; 58:3516–3522. [PubMed: 2228222]

Budu-Amoako E, Greenwood SJ, Dixon BR, Barkema HW, McClure JT. Foodborne illness associated with *Cryptosporidium* and *Giardia* from livestock. J Food Prot. 2011; 74:1944–1955. [PubMed: 22054199]

Chen Y, Riley DJ, Zheng L, Chen PL, Lee WH. Phosphorylation of the mitotic regulator protein Hec1 by Nek2 kinase is essential for faithful chromosome segregation. J Biol Chem. 2002; 277:49408–49416. [PubMed: 12386167]

Chen Y, Chen CF, Chiang HC, Pena M, Polci R, Wei RL, Edwards RA, Hansel DE, Chen PL, Riley DJ. Mutation of NIMA-related kinase 1 (NEK1) leads to chromosome instability. Mol Cancer. 2011a; 10:5. [PubMed: 21214959]

Chen Y, Chen CF, Riley DJ, Chen PL. Nek1 kinase functions in DNA damage response and checkpoint control through a pathway independent of ATM and ATR. Cell Cycle. 2011b; 10:655–663. [PubMed: 21301226]

Davids BJ, Williams S, Lauwaet T, Palanca T, Gillin FD. *Giardia lamblia* aurora kinase: a regulator of mitosis in a binucleate parasite. Int J Parasitol. 2008; 38:353–369. [PubMed: 17964578]

Davids BJ, Gilbert MA, Liu Q, Reiner DS, Smith AJ, Lauwaet T, Lee C, McArthur AG, Gillin FD. An atypical proprotein convertase in *Giardia lamblia* differentiation. Mol Biochem Parasitol. 2011; 175:169–180. [PubMed: 21075147]

Dawson SC, Sagolla MS, Mancuso JJ, Woessner DJ, House SA, Fritz-Laylin L, Cande WZ. Kinesin-13 regulates flagellar, interphase, and mitotic microtubule dynamics in *Giardia intestinalis*. Eukaryot Cell. 2007; 6:2354–2364. [PubMed: 17766466]

Dawson SC, House SA. Life with eight flagella: flagellar assembly and division in *Giardia*. Curr Opin Microbiol. 2010; 13:480–490. [PubMed: 20580308]

DeLuca JG, Howell BJ, Canman JC, Hickey JM, Fang G, Salmon ED. Nuf2 and Hec1 are required for retention of the checkpoint proteins Mad1 and Mad2 to kinetochores. Curr Biol. 2003; 13:2103–2109. [PubMed: 14654001]

Du J, Cai X, Yao J, Ding X, Wu Q, Pei S, Jiang K, Zhang Y, Wang W, Shi Y, Lai Y, Shen J, Teng M, Huang H, Fei Q, Reddy ES, Zhu J, Jin C, Yao X. The mitotic checkpoint kinase NEK2A regulates kinetochore microtubule attachment stability. Oncogene. 2008; 27:4107–4114. [PubMed: 18297113]

Faragher AJ, Fry AM. Nek2A kinase stimulates centrosome disjunction and is required for formation of bipolar mitotic spindles. Mol Biol Cell. 2003; 14:2876–2889. [PubMed: 12857871]

Fry AM, Schultz SJ, Bartek J, Nigg EA. Substrate specificity and cell cycle regulation of the Nek2 protein kinase, a potential human homolog of the mitotic regulator NIMA of *Aspergillus nidulans*. J Biol Chem. 1995; 270:12899–12905. [PubMed: 7759549]

Fry AM. The Nek2 protein kinase: a novel regulator of centrosome structure. Oncogene. 2002; 21:6184–6194. [PubMed: 12214248]

Fu G, Ding X, Yuan K, Aikhionbare F, Yao J, Cai X, Jiang K, Yao X. Phosphorylation of human Sgo1 by NEK2A is essential for chromosome congression in mitosis. Cell Res. 2007; 17:608–618. [PubMed: 17621308]

Hanks SK, Hunter T. Protein kinases 6. The eukaryotic protein kinase superfamily: kinase (catalytic) domain structure and classification. FASEB J. 1995; 9:576–596. [PubMed: 7768349]

Johnson LS, Eddy SR, Portugaly E. Hidden Markov model speed heuristic and iterative HMM search procedure. BMC Bioinformatics. 2010; 11:431. [PubMed: 20718988]

Keister DB. Axenic culture of *Giardia lamblia* in TYI-S-33 medium supplemented with bile. Trans R Soc Trop Med Hyg. 1983; 77:487–488. [PubMed: 6636276]

King RW, Glotzer M, Kirschner MW. Mutagenic analysis of the destruction signal of mitotic cyclins and structural characterization of ubiquitinated intermediates. Mol Biol Cell. 1996; 7:1343–1357. [PubMed: 8885231]

Kramer MH, Herwaldt BL, Craun GF, Calderon RL, Juranek DD. Surveillance for waterborne-disease outbreaks--United States, 1993–1994. MMWR CDC Surveill Summ. 1996; 45:1–33. [PubMed: 8600346]

Lauwaet T, Davids BJ, Torres-Escobar A, Birkeland SR, Cipriano MJ, Preheim SP, Palm D, Svard SG, McArthur AG, Gillin FD. Protein phosphatase 2A plays a crucial role in *Giardia lamblia* differentiation. Mol Biochem Parasitol. 2007; 152:80–89. [PubMed: 17204341]

Lauwaet T, Smith AJ, Reiner DS, Romijn EP, Wong CC, Davids BJ, Shah SA, Yates JR 3rd, Gillin FD. Mining the *Giardia* genome and proteome for conserved and unique basal body proteins. Int J Parasitol. 2011; 41:1079–1092. [PubMed: 21723868]

Liu Q, Hirohashi Y, Du X, Greene MI, Wang Q. Nek2 targets the mitotic checkpoint proteins Mad2 and Cdc20: a mechanism for aneuploidy in cancer. Exp Mol Pathol. 2010; 88:225–233. [PubMed: 20034488]

Liu S, Lu W, Obara T, Kuida S, Lehoczky J, Dewar K, Drummond IA, Beier DR. A defect in a novel Nek-family kinase causes cystic kidney disease in the mouse and in zebrafish. Development. 2002; 129:5839–5846. [PubMed: 12421721]

Lou Y, Yao J, Zereshki A, Dou Z, Ahmed K, Wang H, Hu J, Wang Y, Yao X. NEK2A interacts with MAD1 and possibly functions as a novel integrator of the spindle checkpoint signaling. J Biol Chem. 2004; 279:20049–20057. [PubMed: 14978040]

Mahjoub MR, Qasim Rasi M, Quarmby LM. A NIMA-related kinase, Fa2p, localizes to a novel site in the proximal cilia of *Chlamydomonas* and mouse kidney cells. Mol Biol Cell. 2004; 15:5172–5186. [PubMed: 15371535]

Malumbres M, Barbacid M. Cell cycle kinases in cancer. Curr Opin Genet Dev. 2007; 17:60–65. [PubMed: 17208431]

Manning G, Reiner DS, Lauwaet T, Dacre M, Smith A, Zhai Y, Svard S, Gillin FD. The minimal kinome of *Giardia lamblia* illuminates early kinase evolution and unique parasite biology. Genome Biol. 2011; 12:R66. [PubMed: 21787419]

Marti M, Regos A, Li Y, Schraner EM, Wild P, Muller N, Knopf LG, Hehl AB. An ancestral secretory apparatus in the protozoan parasite *Giardia intestinalis*. J Biol Chem. 2003; 278:24837–24848. [PubMed: 12711599]

Morrison HG, McArthur AG, Gillin FD, Aley SB, Adam RD, Olsen GJ, Best AA, Cande WZ, Chen F, Cipriano MJ, Davids BJ, Dawson SC, Elmendorf HG, Hehl AB, Holder ME, Huse SM, Kim UU, Lasek-Nesselquist E, Manning G, Nigam A, Nixon JE, Palm D, Passamaneck NE, Prabhu A, Reich CI, Reiner DS, Samuelson J, Svard SG, Sogin ML. Genomic minimalism in the early diverging intestinal parasite *Giardia lamblia*. Science. 2007; 317:1921–1926. [PubMed: 17901334]

Nohynkova E, Tumova P, Kulda J. Cell division of *Giardia intestinalis*: flagellar developmental cycle involves transformation and exchange of flagella between mastigonts of a diplomonad cell. Eukaryot Cell. 2006; 5:753–761. [PubMed: 16607022]

O'Regan L, Blot J, Fry AM. Mitotic regulation by NIMA-related kinases. Cell Div. 2007; 2:25. [PubMed: 17727698]

Palm D, Weiland M, McArthur AG, Winiecka-Krusnell J, Cipriano MJ, Birkeland SR, Pacocha SE, Davids B, Gillin F, Linder E, Svard S. Developmental changes in the adhesive disk during *Giardia* differentiation. Mol Biochem Parasitol. 2005; 141:199–207. [PubMed: 15850703]

Parker JD, Bradley BA, Mooers AO, Quarmby LM. Phylogenetic analysis of the Neks reveals early diversification of ciliary-cell cycle kinases. PLoS One. 2007; 2:e1076. [PubMed: 17957258]

Pradel LC, Bonhivers M, Landrein N, Robinson DR. NIMA-related kinase TbNRKC is involved in basal body separation in *Trypanosoma brucei*. J Cell Sci. 2006; 119:1852–1863. [PubMed: 16608878]

Quarmby LM, Mahjoub MR. Caught Nek-ing: cilia and centrioles. J Cell Sci. 2005; 118:5161–5169. [PubMed: 16280549]

Rechsteiner M, Rogers SW. PEST sequences and regulation by proteolysis. Trends Biochem Sci. 1996; 21:267–271. [PubMed: 8755249]

Reiner DS, McCaffery M, Gillin FD. Sorting of cyst wall proteins to a regulated secretory pathway during differentiation of the primitive eukaryote, *Giardia lamblia*. Eur J Cell Biol. 1990; 53:142–153. [PubMed: 2076701]

Reininger L, Tewari R, Fennell C, Holland Z, Goldring D, Ranford-Cartwright L, Billker O, Doerig C. An essential role for the Plasmodium Nek-2 Nima-related protein kinase in the sexual development of malaria parasites. J Biol Chem. 2009; 284:20858–20868. [PubMed: 19491095]

Savioli L, Smith H, Thompson A. *Giardia* and *Cryptosporidium* join the 'Neglected Diseases Initiative'. Trends Parasitol. 2006; 22:203–208. [PubMed: 16545611]

Shalom O, Shalva N, Altschuler Y, Motro B. The mammalian Nek1 kinase is involved in primary cilium formation. FEBS Lett. 2008; 582:1465–1470. [PubMed: 18387364]

Tumova P, Kulda J, Nohynkova E. Cell division of *Giardia intestinalis*: assembly and disassembly of the adhesive disc, and the cytokinesis. Cell Motil Cytoskeleton. 2007; 64:288–298. [PubMed: 17205565]

Ward HD, Lev BI, Kane AV, Keusch GT, Pereira ME. Identification and characterization of taglin, a mannose 6-phosphate binding, trypsin-activated lectin from *Giardia lamblia*. Biochemistry. 1987; 26:8669–8675. [PubMed: 3442682]

Highlights

- The first report of functional analysis of two *Giardia lamblia* Nek kinases.
- Both *Gl*Neks have dynamic re-localization during the cell cycle.
- Over-expression of inactive Nek1 delays parental disk disassembly during the cell cycle.
- Over-expression of wild type Nek1 or inactive Nek2 inhibits excystation.

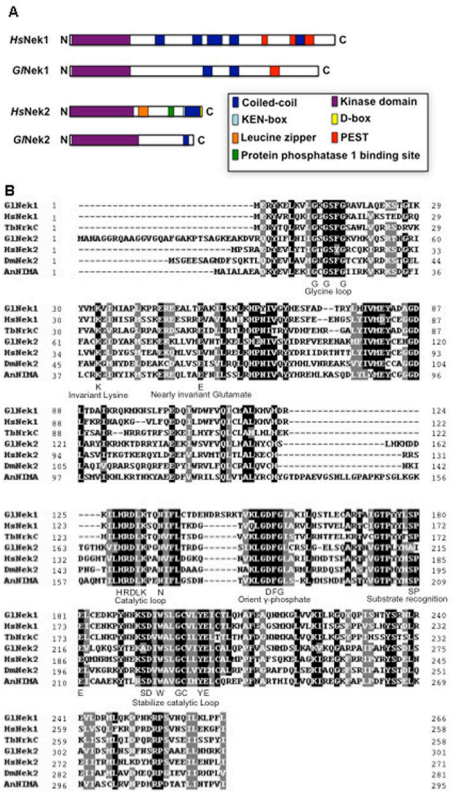

Fig. 1.

Domain and sequence analyses of *Giardia lamblia* NIMA-related serine/threonine kinases, *Gl*Nek1 and *Gl*Nek2. (A) Domains of *Gl*Nek1 (Gl50803_92498), *Gl*Nek2 (Gl50803_5375), human *Hs*Nek1 (Q96PY6) and *Hs*Nek2 (P51955) proteins are color coded as shown in the box. (B) The kinase domains of *Gl*Nek1 and *Gl*Nek2 contain highly conserved kinase sub-domains. Amino acids conserved in more than 75% of sequences are highlighted in black and similar residues are shaded grey. Several critical sub-domains are indicated. *Hs*Nek1 (Q96PY6), *Hs*Nek2 (P51955), *Trypanosoma brucei Tb*NrkC (DQ054526), *Drosophila melanogaster Dm*Nek2 (NM_132187), and *Aspergillus nidulans An*NIMA (P11837) were compared in this alignment.

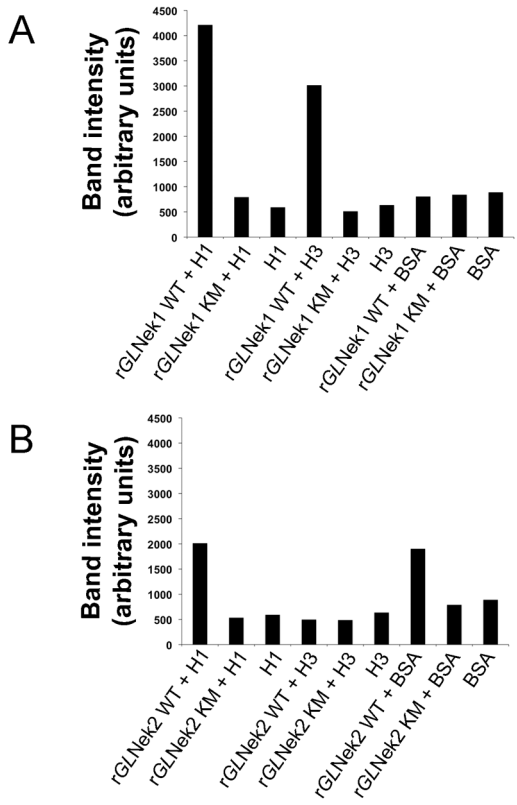

Fig. 2.

Wild type recombinant *Giardia lamblia* NIMA-related serine/threonine kinases, *Gl*Nek1 and *Gl*Nek2, proteins are active in vitro. Bar graphs illustrate the band intensities of the substrates H1, H3 or BSA after incubation in the presence of wild type (WT) or mutant (KM) recombinant *Gl*Nek1 (r*Gl*Nek1) (A) or r*Gl*Nek2 (B). Reactions containing only H1, H3 or BSA substrates without wild type or mutant kinases were used as background controls.

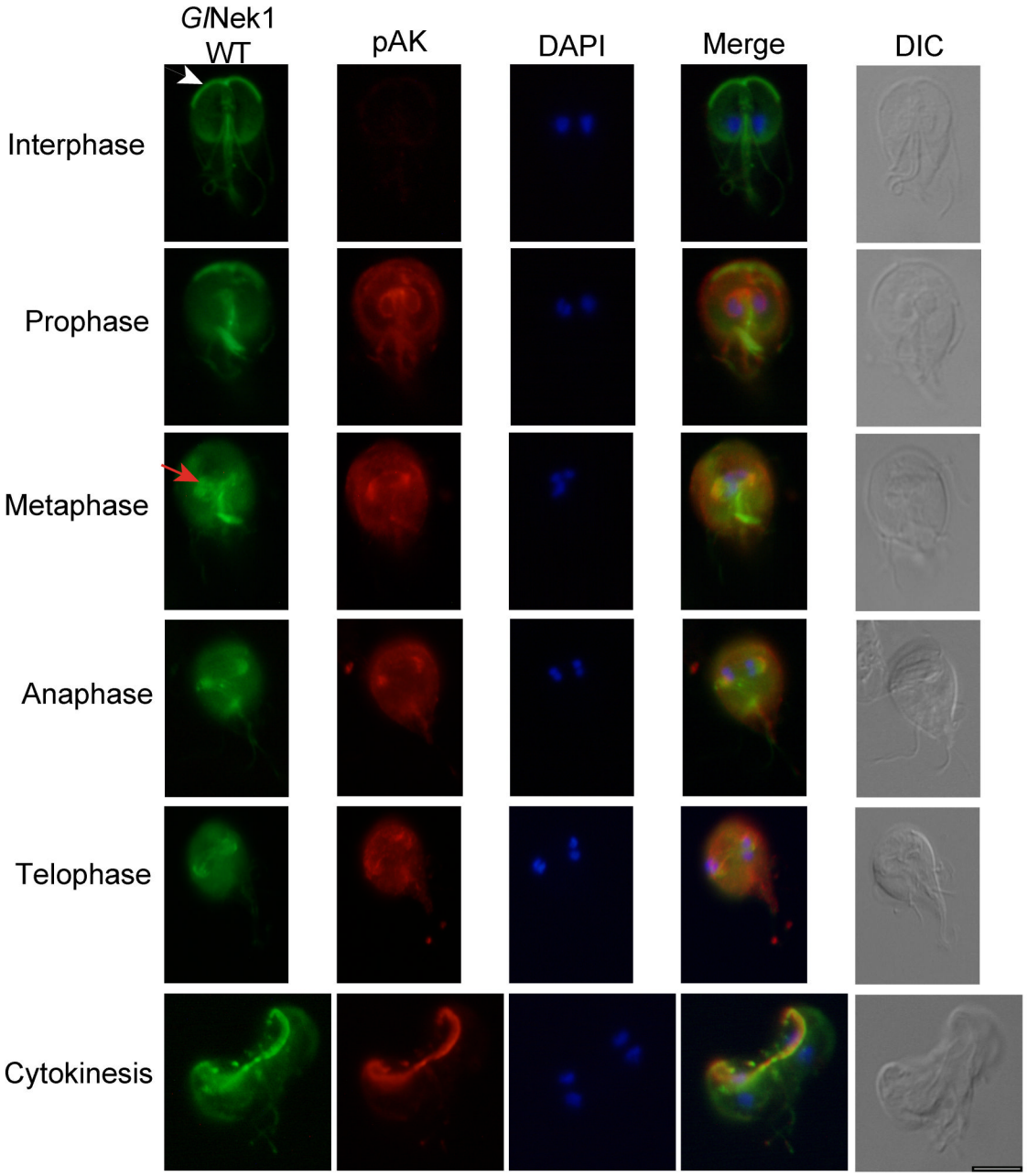

Fig. 3.

Giardia lamblia NIMA-related serine/threonine kinase 1 (*Gl*Nek1) partially co-localizes with phosphorylated Aurora kinase during mitosis. Trophozoites expressing wild type *Gl*Nek1 under the control of its own promoter were co-stained with antibodies against the HA-tag and phosphorylated Aurora Kinase (pAK). DAPI illustrates the localization of the nuclei. The arrowhead indicates the anterior axonemes/paraflagellar rods. The arrow indicates the re-organized basal bodies. The corresponding differential interference contrast (DIC) image is shown. Bar = 10 μm.

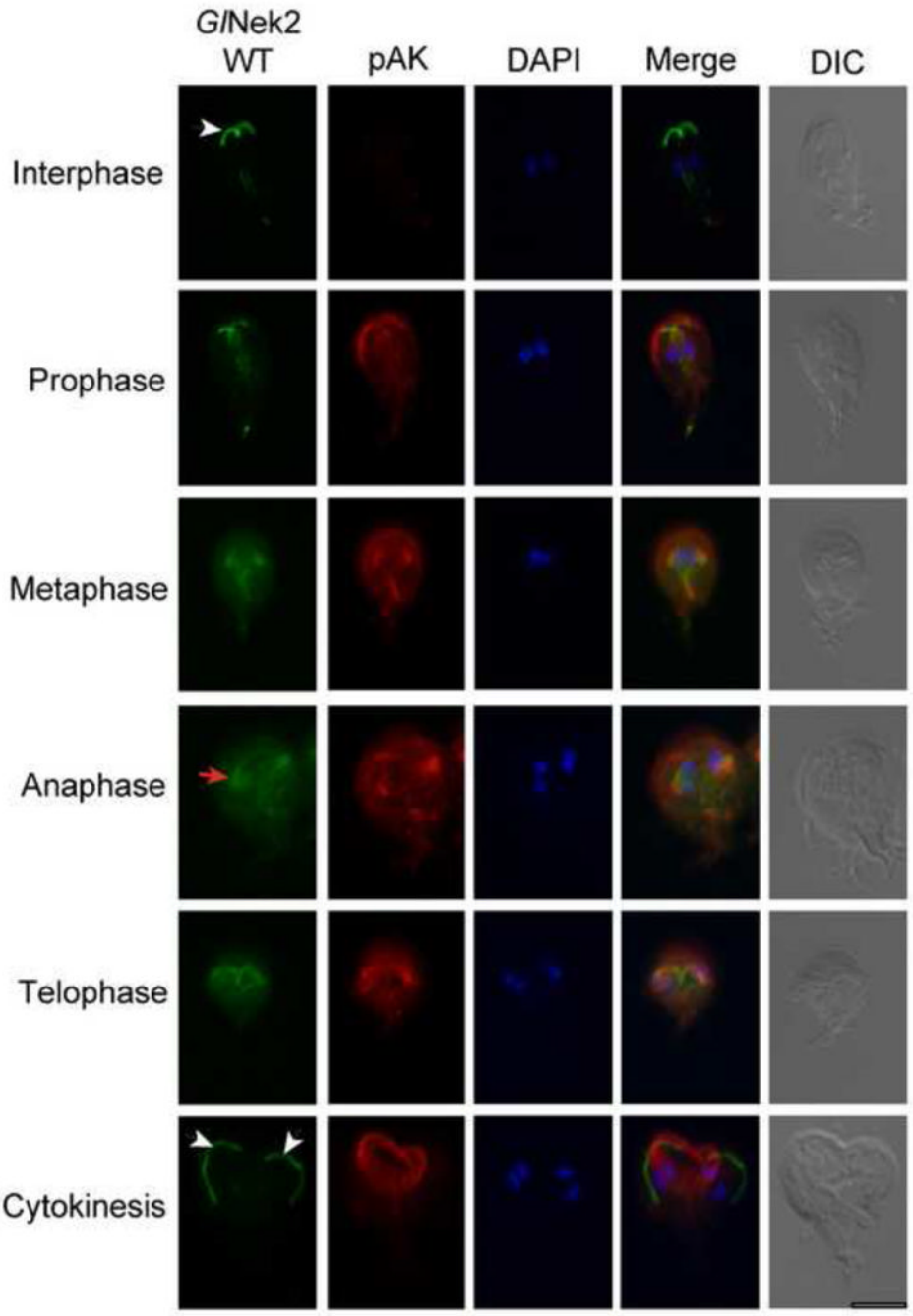

Fig. 4.

Giardia lamblia NIMA-related serine/threonine kinase 2 (*Gl*Nek2) localizes to the spindle poles and spindle apparatus during the cell cycle. Trophozoites expressing HA-tagged *Gl*Nek2-wild type (WT) under the control of its own promoter were co-stained with antibodies against the HA-tag and phosphorylated Aurora Kinase (pAK). DAPI illustrates the localization of the nuclei. The arrowheads indicate the anterior axonemes/paraflagellar rods. The arrow indicates the re-organized basal bodies. The corresponding differential interference contrast (DIC) image is shown. Bar = 10 μm.

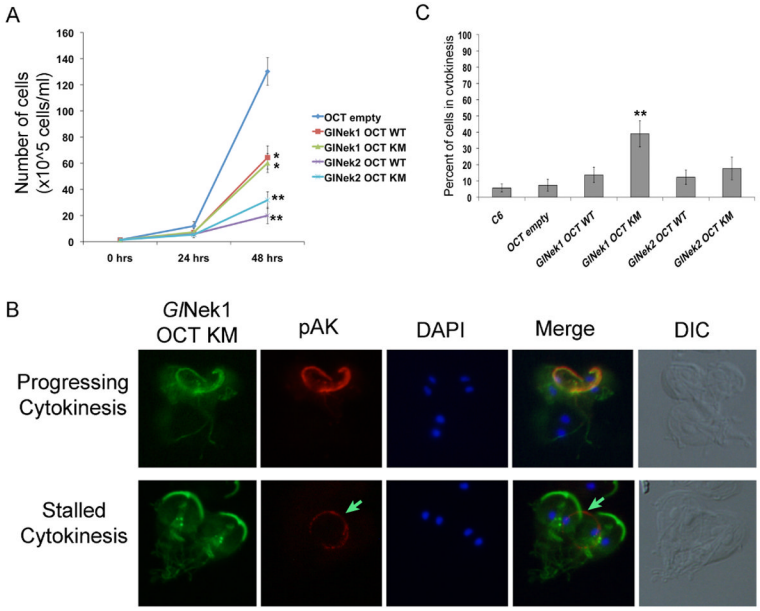

Fig. 5.

Effect of *Giardia lamblia* NIMA-related serine/threonine kinases, *Gl*Nek1 and *Gl*Nek2, on growth and cytokinesis. (A) Equal numbers of cells over-expressing wild type (WT) or mutant (KM) *Gl*Nek 1 or *Gl*Nek2 were inoculated at time 0 and cell growth was determined after 24 and 48 h. * $P < 0.001$, ** $P < 0.0001$. (B) Immunofluorescence analyses of *Gl*Nek-OCT-KM trophozoites with antibodies against the HA-tag and phosphorylated aurora kinase (pAK) show a large proportion of cells with an intact pAK labeled parental disk during cytokinesis ("Stalled Cytokinesis"), indicated by an arrow. Normally, cells in cytokinesis ("Progressing Cytokinesis") display the typical pAK stained and pontoon shaped disassembling parental disk. The corresponding differential interference contrast (DIC) image is shown. (C) Bar graph represents the percentage of cells in cytokinesis per strain. ** $P = 0.0001$. Simple one-way ANOVA was used to determine statistical significances.

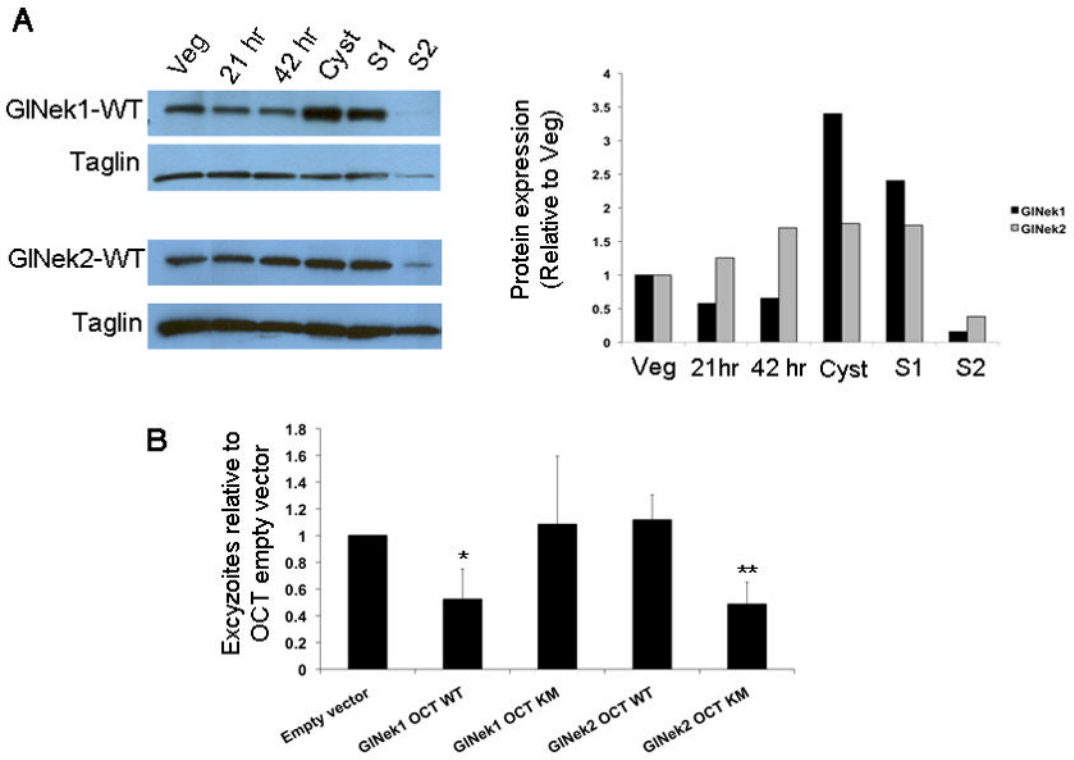

Fig. 6.

Giardia lamblia NIMA-related serine/threonine kinases, *Gl*Nek1 and *Gl*Nek2, in the *Giardia* life cycle. (A) Cell lines expressing *Gl*Nek1-HA or *Gl*Nek2-HA under their own promoter were encysted and excysted. Total protein levels of *Gl*Nek 1 and *Gl*Nek2 from vegetative trophozoites (Veg), 21 h or 42 h encysting trophozoites, cysts and Stage 1 (S1) and Stage 2 (S2) excysting cells were compared by Western blot with the anti-HA-HRP (horseradish peroxidase) antibody. Taglin was used as a protein loading control. The graph shows the band intensities of *Gl*Nek1 and *Gl*Nek2 relative to vegetative cells (Veg). (B) Equal numbers of cysts from cell lines over-expressing wild type (WT) or mutant (KM) *Gl*Nek1 or *Gl*Nek2 were excysted and excyzoites were counted. Bars represent the mean number of excyzoites from three independent experiments from each cell line relative to the empty vector control. * $P < 0.05$, ** $P < 0.005$. Simple one-way ANOVA was used to determine statistical significance.